STUDIA UBB CHEMIA, LXIV, 2, Tom II, 2019 (p. 323-333)
(RECOMMENDED CITATION)
DOI:10.24193/subbchem.2019.2.27

Dedicated to Professor Ioan Bâldea on the Occasion of His 80th Anniversary

STUDY OF S235 STEEL CORROSION PROCESS IN WASTEWATER FROM THE PETROCHEMICAL INDUSTRY

JULIETA DANIELA CHELARU[a], LIANA MARIA MUREŞAN[a*]

ABSTRACT. The aim of this study is to investigate the corrosion behavior of low carbon steel (S235) used in petrochemical industry. The corrosion process was analyzed in simulated wastewater at different values of pH and at different temperatures and also in real wastewater from the exploitation of crude oil from Transylvania, Romania. Two commercial corrosion inhibitors (Nalco 73413 (Nalco Products, USA,) and Galoryl IC20 (ArrMazz Chemicals SAS, USA) were tested at different concentrations. The corrosion behavior was investigated by electrochemical impedance spectroscopy and potentiodynamic polarization measurements. Adsorption of these inhibitors was found to obey Langmuir adsorption isotherm.

Keywords: *electrochemical impedance spectroscopy, polarization curves, steel corrosion, corrosion inhibitors, petroleum industry corrosion.*

INTRODUCTION

Due to the low price, carbon steel is widely used in industry, including the petrochemical industry [1-4]. Because of this, its corrosion has a great impact on the economic environment. Compared to other materials, it has good physical, chemical and mechanical properties, but low corrosion resistance. The main factors contributing to the corrosion of carbon steel in the petrochemical industry are temperature, pressure, but also chemical and microorganism attacks [4-7]. Lately, there are many studies that have focused on finding innovative solutions for the protection against corrosion of carbon steel, with low cost and low environmental impact [3-6]. The most practical method for protecting carbon steel is the use of inhibitors [3, 8-13]. This

[a] *Department of Chemical Engineering, "Babeş-Bolyai" University, 11 Arany Janos St., 400028 Cluj-Napoca, Romania*
** Corresponding author: limur@chem.ubbcluj.ro*

method has proven to be the most economical and efficient. Most commonly used are organic corrosion inhibitors containing heteroatoms, such as nitrogen, sulphur, phosphorus and / or oxygen [8]. There are also studies on the use of green inhibitors [11-13] and commercial inhibitors for the protection of carbon steel [14, 15].

In this context, the purpose of this paper is to investigate the corrosion of low carbon steel (S235) in synthetic solutions simulating wastewater (SWW) from petrochemical industry. The corrosion tests were made at different values of temperature and pH. Also, the corrosion behavior of S235 steel was investigated in wastewater from an exploitation of crude oil (WWCO) from Transylvania, Romania. The tests were made in the absence and in the presence of two commercial inhibitors, Nalco 73413 (Nalco Products, USA) and Galoryl IC20 (produced by ArrMazz Chemicals SAS, USA). The corrosion behavior of S235 steel was investigated by electrochemical methods (electrochemical impedance spectroscopy and polarization measurements).

RESULTS AND DISCUSSION

Corrosion in simulated wastewater

Effect of temperature

In order to determine the corrosion behavior of S235 steel in simulated wastewater (pH 3) at different values of temperature (20 ºC, 30 ºC, 40 ºC), the experiments were started by recording the open circuit potential (OCP) for one hour. Nyquist impedance spectra were recorded immediatly after OCP (results not shown) and the results are presented in Fig. 1.

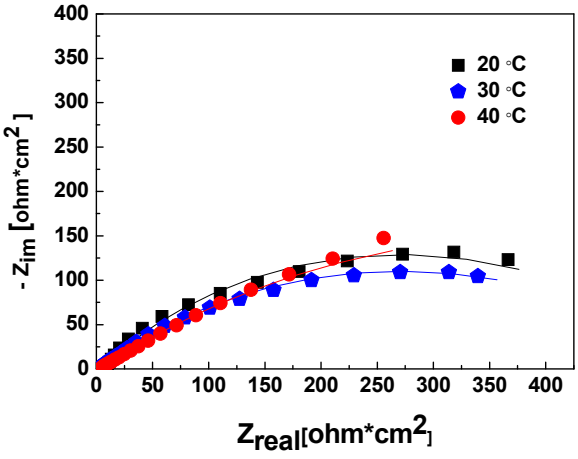

Figure 1. Nyquist plots of the S235 steel dipped in simulated wastewater (pH = 3), at different values of temperature

The spectra ehxibit one depressed capacitive loop. Consequently, the electrical equivalent circuit used to fit the experimental spectra contains besides corrosion solution resistance (R_e), only one R-C couple, presented in Fig. 2. R_{ct} represents the charge transfer resistance and, C_{dl}, the double layer capacity at the steel | electrolyte interface. The data obtained for all samples by using the proposed equivalent electrical circuit are shown in Table 1 (the chi squared (χ^2) values were of order 10^{-4}). The values of C_{dl} were calculated using the equation $C = (R^{1-n}CPE)^{1/n}$, where *CPE* is the constant phase element and *n* reflects the depressed feature of the capacitive loop in Nyquist diagram ($0 < n \leq 1$).

Analyzing the data from Table 1, it can be observed that the polarization resistance (Rp), which is an indicator of corrosion resistance, can be practically assimilated to the charge transfer resistance, and is influenced by temperature. The values of R_p are slightly decreasing with increasing temperature. The highest R_p was observed for T = 20 ºC.

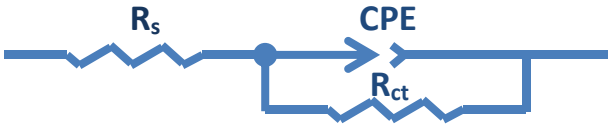

Figure 2. The equivalent electrical circuit used to fit the EIS results

Table 1. The electrochemical impedance data determined by fitting the experimental Nyquist spectra from Figure 1

Temperature [ºC]	Re [Ω·cm²]	R_{ct}[a] [Ω·cm²]	C_{dl}[b] [mF/cm²]	n[c]
20	1.26	537.6	9.078	0.572
30	2.29	533.3	9.433	0.495
40	3.70	418.6	9.544	0.583

a The standard error for Rct values was between 3.24%-5.61%
b The standard error for CPE values was between 2.74%-4.47%
c The standard error for n values was between 0.87%-1.96%

To determine the polarization resistance of the electrodes, linear polarization curves were recorded, in the potential domain of ± 20 mV vs. OCP. The polarization resistance values, for each electrode, were calculated as the inverse of the slope of each curve (Table 2). The largest Rp was observed also at 20 ºC. Potentiodynamic polarization curves were recorded in the potential range of ± 200 mV *vs.* OCP (Fig. 3) in order to determine

the corrosion current density (i_{corr}) and the corrosion potential (E_{corr}). The results obtained by Tafel interpretation of the polarization curves are presented in Table 2. Based on these results, it can be seen that the corrosion of S235 steel increased with the rise of temperature, but not significantly and, as expected, the highest corrosion rate is noticed at 40 ^{0}C. The results are in agreement with EIS measurements.

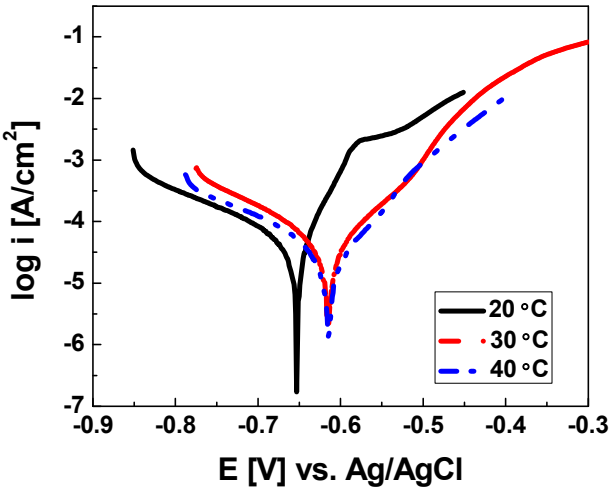

Figure 3. The polarization curves (± 200 mV *vs.* OCP) for the S235 steel immersed in synthetic corrosion solution (pH = 3) at different temperatures; scan rate, 10 mV / min

Table 2. Electrochemical parameters of S235 steel at different temperatures

Temperature	**20 °C**	**30 °C**	**40 °C**
i_{cor} [μA/cm^2]	42.52	49.43	58.04
E_{corr} [mV *vs.* Ag/AgCl/KCl$_{sat}$]	-652	-615	-615
R_p [kΩ cm^2]	0.21	0.19	0.18

Effect of pH

In Fig. 4 are presented the Nyquist plots in case of S235 steel dipped in a simulated wastewater from oil industry at different values of pH (3÷8). The parameters obtained for all samples by using the equivalent electrical circuit from Fig 2 are shown in Table 3. Analyzing the data from Table 3, it can be observed that the corrosion resistance increases at higher pH values. Highest value was obtained at pH 8 (Rp =699.5 [Ω·cm^2]).

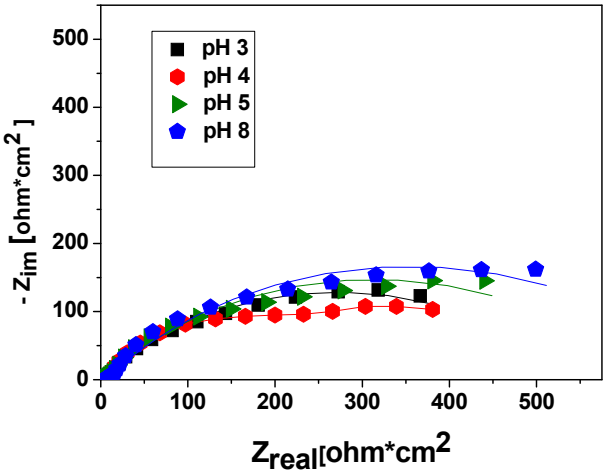

Figure 4. Nyquist plots of the S235 steel dipped in simulated wastewater, at different values of pH

Table 3. The electrochemical impedance parameters estimated by fitting the experimental impedance data from Fig. 6 with the electrical circuit from Fig. 2

pH	R_e [Ω·cm^2]	R_{ct} [Ω·cm^2]	C_{dl} [μF/cm^2]	n
3	1.26	533.3	9.078	0.572
4	2.72	535.3	7.376	0.562
5	3.28	619.9	6.524	0.564
8	5.24	699.5	5.614	0.565

[a] The standard error for Rp values was between 3.40 % - 5.04 %
[b] The standard error for Y_0 values was between 1.68 % - 2.65 %
[c] The standard error for n values was between 1.68 % - 2.65 %

The corrosion currents density and the corrosion potential for the samples studied at different pH values, determined by the Tafel interpretation of the polarization curves from Fig. 5, are shown in Table 4. The results confirm the results obtained through EIS measurements.

Table 4. Electrochemical parameters of S235 steel corrosion at different values of pH

	pH 3	pH 4	pH 5	pH 8
i_{corr} [μA/cm^2]	42.52	37.75	21.73	17.66
E_{corr} [mV *vs.* Ag/AgCl/KCl$_{sat}$]	- 652	- 614	- 535	- 583
Rp [kΩ cm^2]	0.21	0.33	0.48	0.62

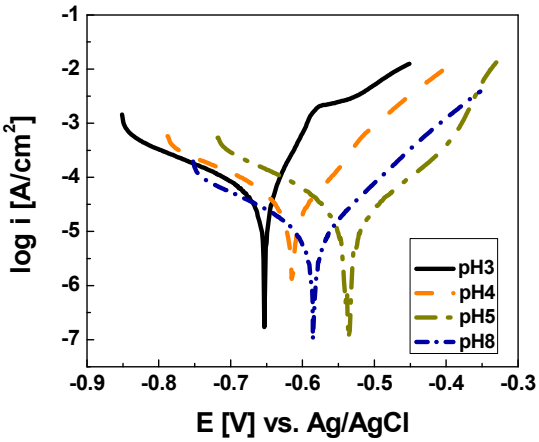

Figure 5. The polarization curves (± 200 mV *vs.* OCP) for the S235 steel immersed in synthetic wastewater at different pH values; scan rate, 10 mV / min

Corrosion in real wastewater

Effect of inhibitors

Fig. 6 shows the Nyquist plots obtained for S235 steel, recorded immediately after OCP monitoring in the real wastewater (pH 8) from an exploitation of crude oil from Transylvania, Romania, without and with different concentrations of two commercial inhibitors (Galoryl IC20, Nalco 73413). It can be seen that all the plots contain depressed semicircles. It was found that the results obtained in the absence and in the presence of inhibitors can be suitably represented using only one time constant circuit. The parameters obtained for all samples are shown in Table 5.

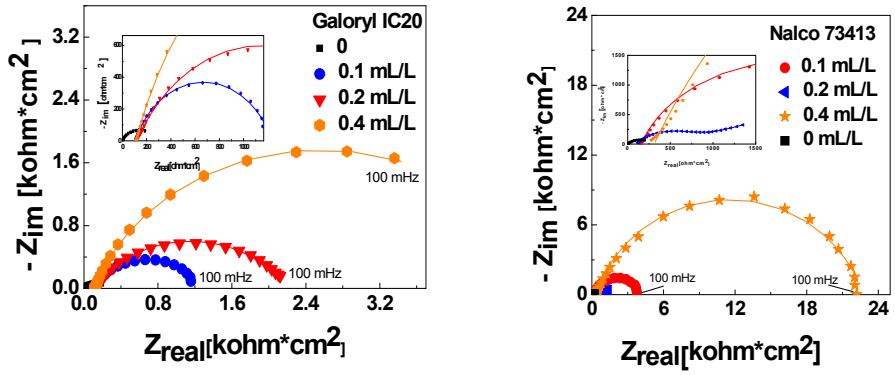

Figure 6. Nyquist plots of the S235 steel dipped in real wastewater (pH 8), from an exploitation of crude oil, at different concentrations of inhibitors; the lines show fitted data

Table 5. The electrochemical impedance parameters estimated by fitting the experimental impedance data from Figure 6

Inhibitor	Conc. [mL / L]	R_e [Ω·cm^2]	R_{ct} [Ω·cm^2]	C_{dl} [μF/cm^2]	n	η [%]
-	0	1.66	280	6.69x10^3	0.611	-
Galoryl IC20	0.1	106	1128	88.06	0.738	75
	0.2	86.35	2626	52.55	0.755	89
	0.4	29.11	9820	44.17	0.398	97
Nalco 73413	0.1	104.60	2143	6.99 x10^3	0.417	90
	0.2	163.70	3756	8.37	0.829	92
	0.4	309.70	22490	2.25	0.800	98

[a] The standard error for *Rp* values was between 1.51 % - 3. 51 %
[b] The standard error for *CPE* values was between 1.19 % - 3.49 %
[c] The standard error for *n* values was between 0.45 % - 1.42 %

Analyzing the data from Table 5, it can be observed that the value of the corrosion resistance depends on the concentrations of inhibitors, which inhibit the corrosion process on the surface of S235 steel. The highest polarization resistance (R_p), was observed at the concentration of 0.4 mL/L in case of both corrosion inhibitors (Table 5).

In Table 5 are presented also the values of the corrosion inhibitors efficiency, determined with the formula: $\eta = \left(\frac{R_p - R_p^0}{R_p} \right) \times 100$ where R_p and R_p^0 are the polarization resistance in presence and in the absence of inhibitors, respectively. As it can be observed, the inhibition is more pronounced in both cases, at higher inhibitors concentration.

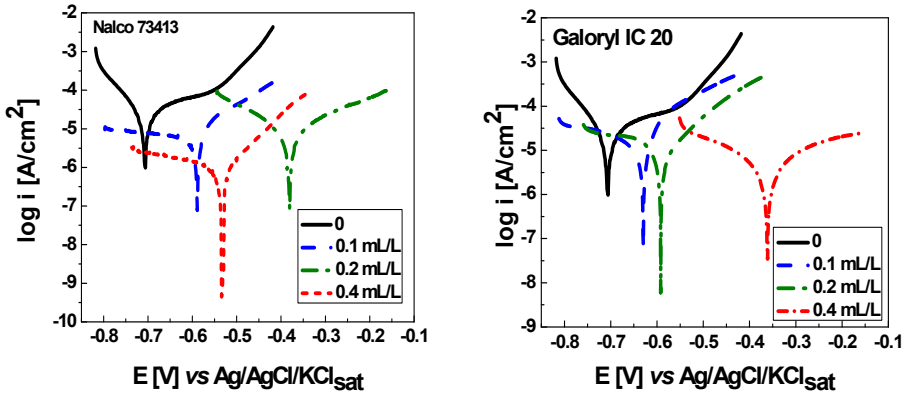

Figure 7. The polarization curves (± 200 mV *vs.* OCP) for the S235 steel immersed in wastewater (pH = 8) at different concentrations of inhibitors; scan rate, 10 mV / min

Table 6. Corrosion process parameters for the examined samples

Inhibitors	Concentrations [mL/L]	E_{corr} [mV vs. Ag/AgCl/KCl$_{sat}$]	i_{corr} [μA/cm^2]	R_p [kΩ*cm^2]	η [%]
-	0	-707	30.33	0.47	-
Nalco 73413	0.1	-596	5.99	2.57	81
	0.2	-385	8.12	3.87	87
	0.4	-533	0.95	30.48	98
Galoryl IC20	0.1	-630	14.38	1.13	58
	0.2	-591	15.95	3.04	84
	0.4	-374	4.49	5.45	91

In order to determine the corrosion currents density and the corrosion potential (E_{corr}), potentiodynamic polarization curves were recorded in the potential range of ± 200 mV *vs.* OCP (Fig. 7). The results are presented in Table 6. The analysis of the data led to the conclusion that in case of both Nalco 73413 and Galoryl IC 20 an increase of corrosion resistance takes place at all inhibitors concentrations.

The highest corrosion resistance and the lowest corrosion current density were noticed at 0.4 mL/L concentration of inhibitors and the best results were noticed in the case of Nalco 73413. This is in agreement with the results obtained from the EIS measurements.

Adsorption isotherm

The efficiencies of the corrosion inhibitors are related to their adsorption ability on the steel surface. The inhibitors reduce the corrosion rate by covering the steel surface with inhibitor molecules. For this purpose, the efficiencies (Table 5 and Table 6), were used to calculate the degree of surface coverage $\theta = \eta / 100$.

In Fig. 8 the linear relationships of C_{in}/θ *versus* C_{in} suggest that the adsorption of both inhibitors (Nalco 73413 and Galoryl IC20) on S235 steel are well described by the Langmuir isotherm: $\frac{C_{in}}{\theta} = \frac{1}{K} + C_{in}$, where K is the adsorption equilibrium constant and C_{in} is the inhibitor concentration (Fig. 8). This kind of isotherm involves the assumption that no interaction between the adsorbed molecules on the electrode surface exists.

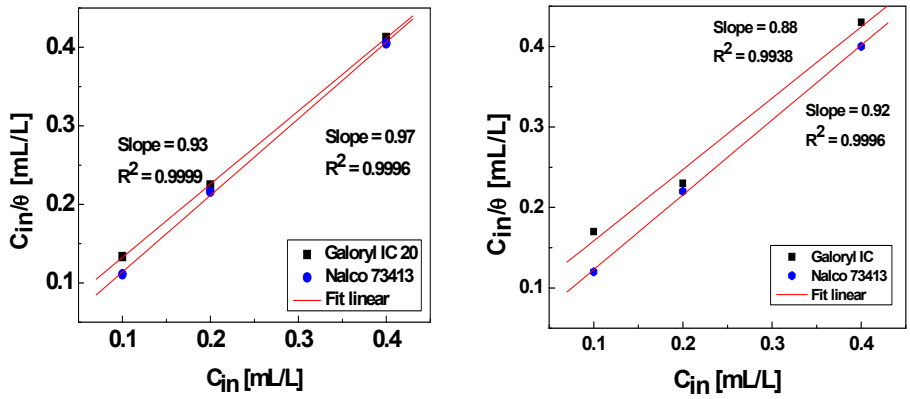

Figure 8. Langmuir adsorption isotherm of the inhibitors by using surface coverage values calculated by a) EIS results and b) Tafel polarization results

CONCLUSIONS

Electrochemical investigations (EIS and potentiodynamic polarization curves measurements) have shown that the corrosion resistance of S235 steel recorded lower values at higher temperature and lower pH values.

When using corrosion inhibitors, the electrochemical results showed that the corrosion resistance improved as their concentration increased. Both used inhibitors exert a good protective effect against steel corrosion in wastewater from petrochemical industry. The best efficiency was noticed when 0.4 mL/L concentration of inhibitors was used (η= 86.61 % for Nalco 73413 and respectively η = 87.07 % for Galoryl IC 20).

Results obtained from EIS and potentiodynamic polarization measurements demonstrated that the adsorption of inhibitors (Nalco 73413, Galoryl IC 20) on S235 steel surface immersed in synthetic and real wastewater from petrochemical industry obeyed Langmuir isotherm and exhibit single-layer adsorption characteristics.

EXPERIMENTAL

Materials and methods

The samples made of S235 steel used for electrochemical tests were disk shaped with 0.8 cm diameter (about 0.5 cm^2 of the surface was exposed to the corrosive solution). Prior tests, the steel samples were

ground using emery papers from # 800 up to # 2000 grades, cleaned with acetone, with distilled water, dried at room temperature, and mounted in Teflon. For electrical contact, a copper road was used.

The commercial corrosion inhibitors used in the experiments were: (i) Nalco 73413 (Nalco Products), (ii) Galoryl IC 20 EU. The inhibitors were dissolved in the corrosive solution at concentrations: 0.1 mL / L, 0.2 mL / L, 0.4mL / L. For corrosion tests, two different solutions were used: (i) an electrolyte that simulated wastewater of high salinity, (pH = 3÷8) and (ii) a wastewater from petroleum industry (pH = 8) containing besides inorganic ions, oils and hydrocarbs. The composition of the synthetic wastewater is presented in Table 7 [14]. For pH correction, NaOH was used.

Table 7. The composition of the electrolyte used in corrosion tests (pH = 3)

Conc.	Fe^{3+}	Ni^{2+}	Cu^{2+}	Na^{+}	K^{+}	SO_4^{2-}	NO_3^{-}	Cl^{-}
g / L	0.02	0.006	$0.1 \cdot 10^{-3}$	50	5.4	6.64	$0.27 \cdot 10^{-3}$	77.09

For the electrochemical corrosion measurements, a PC – controlled electrochemical analyzer PAR 2273 (Princeton Applied Research, USA) connected to a cell containing three electrodes was used: the working electrode (S235 steel), a counter electrode (platinum) and a reference electrode (Ag/ClAg). The open circuit potential (OCP) for steel immersed in the corrosive solution was monitored during one hour. The EIS measurements were performed with a disturbance voltage of ± 10 mV and frequency ranging from 10^3 – 10^{-3} Hz and the results were fited using the ZSimpWin V3.21 software. In order to determine the corrosion parameters, the potentiodynamic polarization curves were recorded by scanning in a potential range of ± 20 mV and of ± 200 mV *vs.* OCP, with a scan rate of 10 mV / min.

REFERENCES

1. M.N. Ilman, Kusmono, *Case Studies in Engineering Failure Analysis*, **2014**, *2*, 1 - 8.
2. W. Geary, *Case Studies in Engineering Failure Analysis*, **2013**, *1*, 249 - 256.
3. G. Sıgırcık, T. Tüken, M. Erbil, *Applied Surface Science*, **2015**, *324*, 232 - 239.
4. T. Liu, Y. F. Cheng, M. Sharma, G. Voordouw, *Journal of Petroleum Science and Engineering*, **2017**, *156*, 451 - 459.
5. W Zhao, Y. Zou, K. Matsuda, *Corrosion Science*, **2015**, *51*, 761 - 768.

6. R. Xiao a, G. Xiao, B. Huanga, J. F. Qionghui, *Engineering Failure Analysis*, **2016**, *68*, 113 - 121.
7. Y. Liu, B. Zhang, Y. Zhang, L. Ma, P. Yang, *Engineering Failure Analysis*, **2016**, *60*, 307 - 315.
8. M. Finšgar, J. Jackson, *Corrosion Science*, **2014**, *86*, 17 - 41.
9. M. Askari, M. Aliofkhazraei, S. Ghaffari, A. Hajizadeh, *Journal of Natural Gas Science and Engineering*, **2018**, *58,* 92 - 114.
10. Y. Zhu, M. L. Free, R. Woollam, W. Durnie, *Progress in Materials Science*, **2017**, *90*, 159 - 223.
11. A. A. Olajire, *Journal of Molecular Liquids*, **2017**, *248*, 775 - 808.
12. K. Haruna, I.B. Obot, N.K. Ankahc, A.A. Sorour, T.A. Saleha, *Journal of Molecular Liquids*, **2018**, *264*, 515 - 525.
13. Gh. Golestani, M. Shahidi, D. Ghazanfari, *Applied Surface Science* **2014**, *308*, 347 – 362.
14. J. D. Chelaru, D. Aylakov, L. M. Mureşan, *Studia UBB Chemia*, **2017**, *62*(4, Tom II), 357 - 368.
15. H. Essom, *Journal of Materials and Environmental Science*, **2015**, *6* (7) 1850 – 1857.